

Osteoarthritis and Cartilage



Reduced chondrocyte proliferation, earlier cell cycle exit and increased apoptosis in neuronal nitric oxide synthase-deficient mice

Q. Yan ^{†‡}, Q. Feng [†], F. Beier ^{†‡*}

[†] Department of Physiology and Pharmacology, Schulich School of Medicine and Dentistry, University of Western Ontario, London, ON, Canada, N6A 5C1

[‡] Children's Health Research Institute, London, ON, Canada

ARTICLE INFO

Article history:

Received 28 March 2011

Accepted 24 November 2011

Keywords:

Nitric oxide

Neuronal nitric oxide synthase

Chondrocyte proliferation

Endochondral bone formation

SUMMARY

Objective: Nitric oxide (NO) has been implicated in the local regulation of bone metabolism. However, the contribution made by specific nitric oxide synthase (NOS) enzymes to skeletal development is unclear. The objective of this study was to examine the effects of inactivation of neuronal nitric oxide synthase (nNOS) on cartilage development in mice.

Design: Mice carrying a null mutation in the nNOS gene were used to address our objectives. Histological staining, immunohistochemistry and *in situ* analyses were employed along with real-time reverse transcriptase – polymerase chain reaction (RT-PCR).

Results: nNOS-null mice show transient growth retardation and shorter long bones. nNOS-deficient growth plates show a reduction in replicating cells. Reduced chondrocyte numbers may in part be due to slower cell cycle progression and premature cell cycle exit caused by decreased cyclin D1 and increased p57 expression in mutants. In addition, apoptosis was increased as shown by increased cleaved-caspase 3 staining in hypertrophic chondrocytes in mutants. Real-time PCR demonstrated that expression of early chondrocyte markers such as Sox genes was reduced in mutant mice, while expression of prehypertrophic markers such as ROR α was increased. Histological sections also demonstrated thinner cortical bone, fewer trabeculae and reduced mineralization in mutant mice.

Conclusions: These data identify an important role of nNOS in chondrocyte proliferation and endochondral bone growth and demonstrate that nNOS coordinates cell cycle exit and chondrocyte differentiation in cartilage development.

© 2011 Osteoarthritis Research Society International. Published by Elsevier Ltd. All rights reserved.

Introduction

NO is a small signaling molecule with important regulatory effects in many tissues. It can function as an intracellular messenger, an autacoid, a paracrine substance, or a neurotransmitter¹. The versatile functions of NO stem from the chemical properties of the compound. NO is a gaseous uncharged free radical with an unshared electron that can react with many molecules and proteins to regulate biological processes². Because it is uncharged, it can freely diffuse to the surrounding cells, making it ideal as a signaling molecule³. In most processes, NO activates soluble guanylyl cyclase (GC), resulting in increased levels of the intracellular secondary messenger cyclic guanosine monophosphate

(cGMP)^{1,2}, but other modes of signaling such as protein nitrosylation also contribute to the biological effects of NO^{2,4}. Different cells and tissues have different abilities to produce NO. In general, low levels of NO are produced from constitutive NOSs, (endothelial NOS/eNOS and neuronal NOS/nNOS) and high levels of NO stem from inducible nitric oxide synthase (iNOS). The ultimately effects of NO are determined by its concentration, its source, and the availability of molecules in the microenvironment that it can react with. Over years NO has been known to regulate bone cell metabolism, bone remodeling and chondrocyte physiology in osteoarthritis (OA)^{3,5,6}, but the contributions made by specific NOS enzymes to bone growth and development are unclear^{7,8}. In light of the prevalent connections between chondrocyte differentiation and the pathogenesis of OA⁹, and the well-known roles of NO in OA, the elucidation of the roles of individual NOS genes in cartilage development is of great importance.

Formation of the skeleton is achieved through two independent mechanisms: intramembranous and endochondral ossification¹⁰. Endochondral bone formation is a precisely regulated process and

* Address correspondence and reprint requests to: F. Beier, Department of Physiology and Pharmacology, Schulich School of Medicine and Dentistry, University of Western Ontario, London, ON, Canada, N6A 5C1. Tel: 519-661-2111x85344; Fax: 519-661-3827.

E-mail address: fbeier@uwo.ca (F. Beier).

responsible for the formation of most bones in the adult skeleton. It involves the steps of chondrogenesis, chondrocyte proliferation, differentiation, and hypertrophy and eventually replacement of cartilage tissue by bone tissue and bone marrow^{3,10–13}. During postnatal development, proliferation and hypertrophy occur in a controlled fashion in the cartilage growth plate that determines the final length of the adult bone. Within the growth plate, chondrocytes are organized in distinguished zones (resting, proliferating, prehypertrophic and hypertrophic zones) based on their morphologic shapes and gene expression patterns¹¹. If any steps during this process are not properly regulated, skeletal diseases will result, such as different types of chondrodysplasias¹⁴. In addition, links between skeletal developmental and the pathogenesis of OA are becoming evident. For example, both disturbances of normal endochondral ossification and ectopic initiation of chondrocyte hypertrophy in articular cartilage have been implicated in OA^{15,16}. Thus, investigations into the mechanisms controlling normal cartilage development are essential for our understanding of OA pathogenesis.

We recently described cartilage development in *eNOS*- and in *iNOS*-deficient mice that both display reduced bone growth^{17,18}. This effect appears to be due to a chondrocyte-autonomous role of *eNOS* in chondrocyte proliferation. However, *nNOS* mRNA levels were upregulated in *eNOS*-null chondrocytes, suggesting that *nNOS* partially compensates for the loss of *eNOS*. *nNOS* knockout (KO) mice have been found to be viable, have enlarged stomachs due to pyloric muscle hypertrophy, exhibit insulin resistance and resistance to neural damage as the result of stroke induced by middle cerebral artery ligation¹⁹. *nNOS* expression has been detected during skeletal development and fracture healing, and previous studies showed reduced bone remodeling with a significant reduction in osteoblast and osteoclast numbers in *nNOS*-deficient mice¹⁹. However, the exact mechanisms and functions of *nNOS* in earlier stages of skeletal development have not been described. In this study, we investigated the effects of *nNOS* deficiency on cartilage development and endochondral bone formation.

Materials and methods

Antibodies and reagents

All reagent materials and general chemicals were obtained from Invitrogen, Sigma or VWR unless otherwise stated. The following antibodies were employed in this study: Kip2/p57 #sc8298 (rabbit antibody against human protein), ROR α #sc28612 (rabbit antibody against human protein), activating transcription factor 3 (ATF3) #sc188 (rabbit antibody against human protein), Sox9 #sc-17340 (goat antibody against human protein), c-Fos #sc-52 (rabbit antibody against human protein), Goat-anti-mouse #sc2005, Goat-anti-rabbit #sc2004 (all from Santa Cruz Biotechnology); Cyclin D1 (SP4) #9104-S1 (rabbit antibody against human, mouse and rat proteins; NeoMarkers Inc.); proliferating cell nuclear antigen (PCNA) #2586 (mouse antibody against human, mouse and rat proteins; Cell Signaling Inc.).

Mouse breeding and genotyping

Mice with a deletion of the *nNOS* gene (Stock #2986) and control mice in the C57/BL6 background were obtained from Jackson Laboratory (Bar Harbor, ME), and exposed to a 12-h light-dark cycle and fed tap water and regular chow *ad libitum*¹⁹. All procedures involving animals were approved by the University of Western Ontario Animal Care and Use Committee. For PCR genotyping, tail snips were used to prepare DNA for PCR analysis. PCR genotyping was performed by simultaneous amplification of the wild type and

null *nNOS* alleles as described^{9,19}. PCR fragments were analyzed by agarose gel electrophoresis.

Histology and immunohistochemistry

After dissection of mice, bones were rinsed in PBS, fixed in 4% paraformaldehyde (PFA) overnight, placed in 10% formalin solution and sent for embedding and sectioning into 4 μ m sections at the Molecular Pathology Core Facility at the Robarts Research Institute (London, Ontario, Canada). Following sectioning, bones were stained with hematoxylin and eosin or safranin O/fast green using standard protocols^{20,21} or used for immunohistochemistry as described below.

For immunohistochemistry, sections unstained prior to use were dewaxed and incubated in 3% H₂O₂ for 15 min at room temperature, followed by boiling for 20 min in 10 mM sodium citrate (pH 6.0) and blocking with 5% goat serum at room temperature for 30 min, as described^{17,21–23}. Sections were incubated with primary antibody overnight at 4°C and secondary antibodies according to the manufacturers' recommendations. After washing, sections were incubated for 1–10 min with DAB (3,3'-diaminobenzidine tetrahydrochloride) substrate solution (Dako North America, Inc.), washed and mounted. All images were taken at room temperature with a Retiga EX camera connected to a Leica DMRA2 microscope using OpenLab 4.0.4 software. For cell counts in sections, all cells and cells positive for staining with primary antibody were counted from three different areas of one section. Sections from at least three mice per genotype, and at least three sections from every mouse, were analyzed, and averages and standard deviation from all counts/genotype are shown.

RNA isolation and real-time RT-PCR

Total RNA was isolated from epiphyseal cartilage of long bone from newborn mice using TRIzol (Invitrogen), according to the manufacturer's recommendations. TaqMan real-time PCR was performed as described^{21,24} with primers and probe sets from Applied Biosystems (Sox5 Mm00488381_m1; Sox6 Mm00488393_m1; Sox9 Mm00448840_m1; P57 Mm00438170_m1; MMP13 Mm00439495_m1; Igf1 Mm00439560_m1; *Gapdh* Mm9999915_g1). Data were normalized to *Gapdh* mRNA levels and represent averages and SEM from direct comparison of mutant and control littermates from three different crosses.

Statistical analysis

All experiments were performed with at least three independent litters (each litter representing one independent experiment). Statistical significance of experiments was determined by a one-way analyses of variance (ANOVA) with Bonferroni post test using GraphPad Prism version 4.00 for Windows, GraphPad Software, San Diego, California, USA. Data presented in the graph show mean and 95% confidence intervals.

Results

Inactivation of *nNOS* gene results in reduced bone length

We used *nNOS*-deficient mice to address the role of this gene in cartilage development *in vivo*. KO mice were viable and fertile, and the general appearance of stature and gait was unremarkable, but male KO mice appeared more aggressive. Body weight and length were not significantly changed in *nNOS*^{−/−} mice at birth. Growth retardation developed in surviving *nNOS*^{−/−} mice in the postnatal period at day 21–42, as shown by reduced body weight and length [Fig. 1(A)]. Body weight showed significant reduction at postnatal

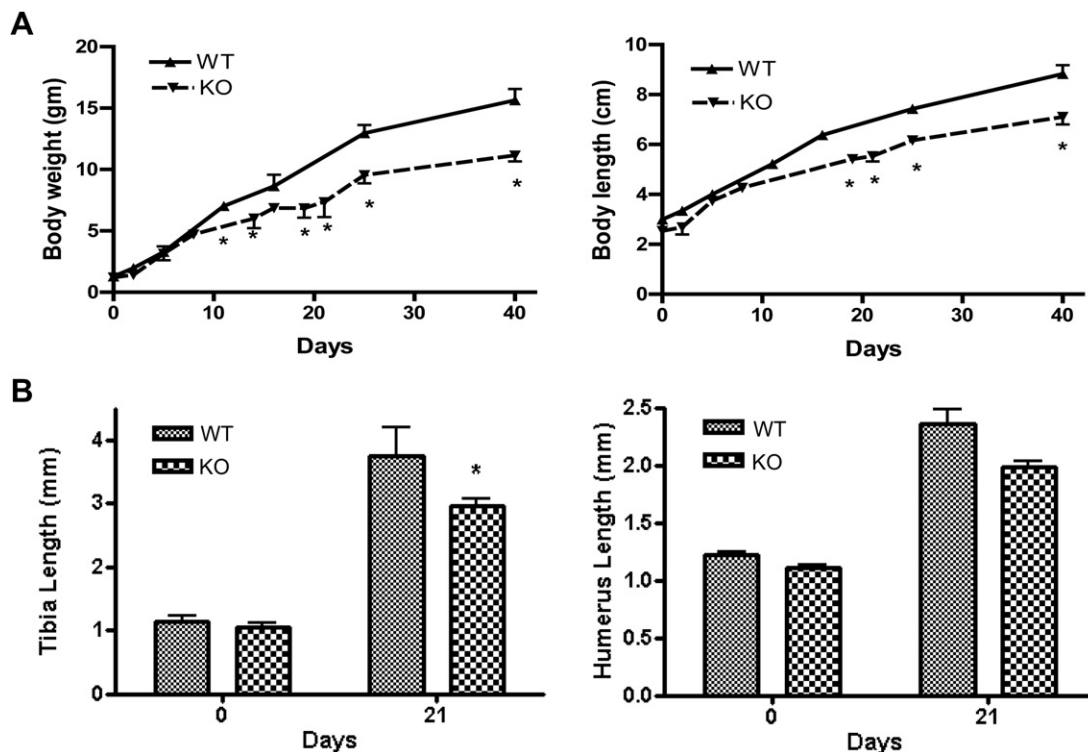


Fig. 1. Loss of *nNOS* results in reduced growth and bone length. Analyses of body weight and length of wild type and *nNOS* homozygote null mice showed that growth retardation developed in *nNOS*-null mice during the first 42 days of their life (A). Measurement of selected individual bones confirmed reduced bone length in tibiae in postnatal day 21 mutant mice (B). At least eight mice per genotype are shown for each data point. (* $P < 0.05$, mean \pm 95% confidence interval) (WT: wild type; KO: knockout).

day 11, before body length was reduced [Fig. 1(A)]. However, analyses at 3-month and 1 year of age demonstrated similar body weight and body length between genotypes (data not shown), suggesting that KO mice catch up during aging. Observation of alcian blue/alizarin red-stained skeletons showed no obvious morphological changes in the axial and appendicular skeleton of mutants (data not shown), but measurement of selected individual bones confirmed reduced bone length in tibiae in mutant mice at postnatal day 21 [Fig. 1(B)].

nNOS deficiency results in reduced chondrocyte proliferation in the growth plate

To elucidate the cellular basis for reduced bone growth, we analyzed growth plate organization at different developmental stages. Growth plates from newborn mutant mice displayed a similar chondrocyte arrangement in resting, proliferative and hypertrophic zones as control mice [Fig. 2(A)]. Measurement of the lengths of resting, proliferating and hypertrophic zones did not show significant differences (data not shown) between genotypes, and cells in the resting and hypertrophic zones of *nNOS*-null mice did not appear markedly different from controls. However, *nNOS*^{-/-} growth plates appeared slightly disorganized with fewer and shorter columns, especially in the proliferative zone in the center of the growth plates. Some cells also appeared to be smaller in size [Fig. 2(A,B)].

Since our mutant mice showed lower cell numbers in the proliferative zone of the growth plate, we next examined chondrocyte proliferation and apoptosis. Immunohistochemical staining for PCNA demonstrated a reduction in positive cells in mutant mice [Fig. 3(A)] which was confirmed by cell counts [Fig. 3(B)]. Reduced cell numbers could also be due to increased cell apoptosis, which we examined by immunohistochemical staining for cleaved

(activated) caspase 3. Staining for cleaved caspase 3 was increased in hypertrophic chondrocytes of mutant mice [Fig. 3(C)].

To elucidate the reason for reduced proliferation in *nNOS*^{-/-} mice, we examined cell cycle protein expression in growth plates. Immunohistochemical staining for cyclin D1, which controls progression through the G1 phase of the cell cycle¹¹, demonstrated a reduced number of positive cells in mutant mice [Fig. 3(D)]. The transcription factor ATF3 acts as a repressor of cyclin D1 transcription in chondrocytes²⁵. Immunohistochemistry demonstrated earlier induction of ATF3 expression in late proliferating chondrocytes and overall stronger ATF3 staining in *nNOS*-deficient growth plates [Fig. 3(E)], suggesting that premature induction of ATF3 expression in mutant mice leads to repression of cyclin D1 transcription and chondrocyte proliferation.

Increased differentiation in *nNOS*-deficient chondrocytes

Since reduced chondrocyte proliferation is often associated with premature cell cycle exit and maturation¹¹, we examined the expression of additional markers of prehypertrophic chondrocytes. Expression of the cell-cycle inhibitor p57, which promotes cell cycle exit and is required for normal chondrocyte differentiation, was found strongly increased by immunohistochemistry in mutant mice [Fig. 4(A)]. Immunohistochemistry also showed a similar increase in the number of cells expressing the transcription factors c-Fos [Fig. 4(B)] and ROR α [Fig. 4(C)], both of which have been implicated in prehypertrophic/hypertrophic chondrocyte-specific gene expression^{26,35}.

nNOS deficiency affects cartilage-specific gene expression

In parallel, we analyzed expression of several cartilage marker genes in the mutant mice by real-time reverse transcriptase - polymerase chain reaction (RT-PCR), using RNA directly extracted

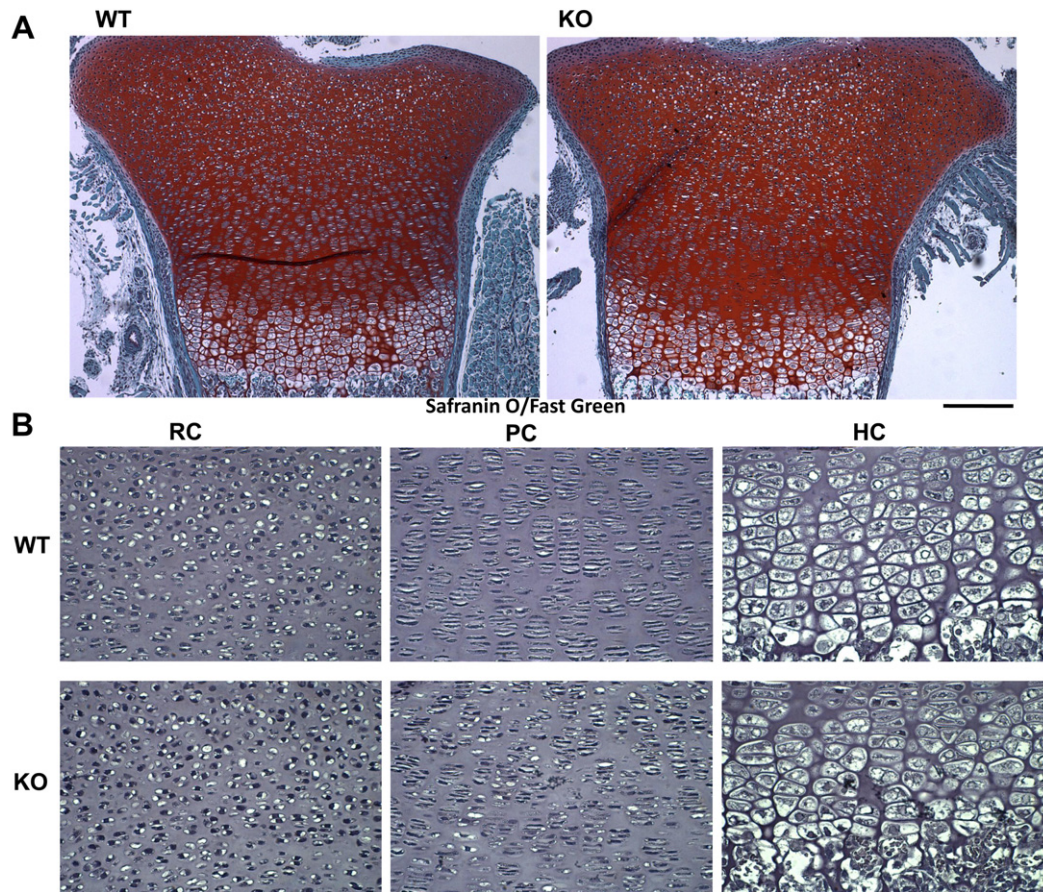


Fig. 2. Lack of *nNOS* causes reduced numbers of proliferating chondrocytes. Safranin O/Fast Green staining of tibia growth plate sections from newborn mice demonstrated similar growth plate architecture in both genotypes (A and B). Detailed analyses of H&E stained sections in the resting, proliferative, and hypertrophic zones showed that the major differences occur in the proliferative zone (B). (RC: resting cells; PC: proliferating cells; HC: Hypertrophic cells). (Scale bar = 200 μ m).

from epiphyseal cartilage. Our results revealed decreased expression for *Sox5* and *Sox6* that are important for many stages of chondrocyte differentiation [Fig. 5(A,B)]. Real-time RT-PCR also demonstrated increased expression of prehypertrophic and hypertrophic markers *p57* and *Mmp13* [Fig. 5(C,D)]. Transcript levels for *Igf1*, which plays an important role in regulating skeletal development and bone remodeling²¹, were also strongly decreased in the mutant mice [Fig. 5(E)]. Interestingly, we also demonstrated upregulated *eNOS* and *iNOS* mRNA levels in the *nNOS* KO cartilage samples [Fig. 5(F,G)].

Loss of nNOS results in reduced trabecular bone and calcium deposition

To analyze whether *nNOS* deficiency had effects on later stages of endochondral ossification, we next examined trabecular bone formation and ossification patterns in mutant mice. Von Kossa staining demonstrated mineralization of trabecular and cortical bone in tibia sections from neonate and postnatal day 21 mice, which was clearly decreased in mutant mice [Fig. 6(A)]. A lack of trabecular structures was also seen by picosirius red staining for fibrillar collagen [Fig. 6(B)], suggesting that these effects are not simply due to delayed mineralization, but to a delay or reduction in bone formation. Secondary ossification centers were advanced in control mice at postnatal day 12, but less advanced in age-matched KO mice, demonstrating that *nNOS* deficiency results in delayed secondary ossification [Fig. 6(C)].

Discussion

The signaling pathways that control growth plate chondrocyte proliferation and differentiation during endochondral ossification are incompletely understood. In this study, we provide evidence for an important role of the *nNOS* gene in these processes. Our data show that genetic ablation of *nNOS* results in reduced chondrocyte proliferation and endochondral bone growth *in vivo*. Analyses of these changes in cellular and molecular levels suggest that these effects are likely due to altered expression of several cell-cycle proteins, such as cyclin D 1 and *p57*, as well as modulation of other genes with known roles in cartilage differentiation, including *Sox* genes, *ROR α* and *c-Fos*.

Although there were no obvious morphological changes in the axial and appendicular skeleton, measurement of individual bone confirmed shorter tibiae and femurs in postnatal day 21 mutant mice. Detailed analyses of *nNOS* null tissue sections revealed several abnormalities, most notably reduced chondrocyte proliferation. *nNOS*-deficient growth plates resemble those we observed in mice lacking the *eNOS* or *iNOS* genes^{17,18} and also share similarities to those in mice deficient for C-type natriuretic peptide (CNP)²⁷. Because both NO and CNP stimulate the production of cGMP via soluble or particulate GCs²⁷, these similarities are not surprising and further document the importance of cGMP signaling in endochondral bone formation. However, it should be noted that a major phenotype of CNP null mice is a reduction in the length of the hypertrophic zone²⁷ that we did not observe here. One

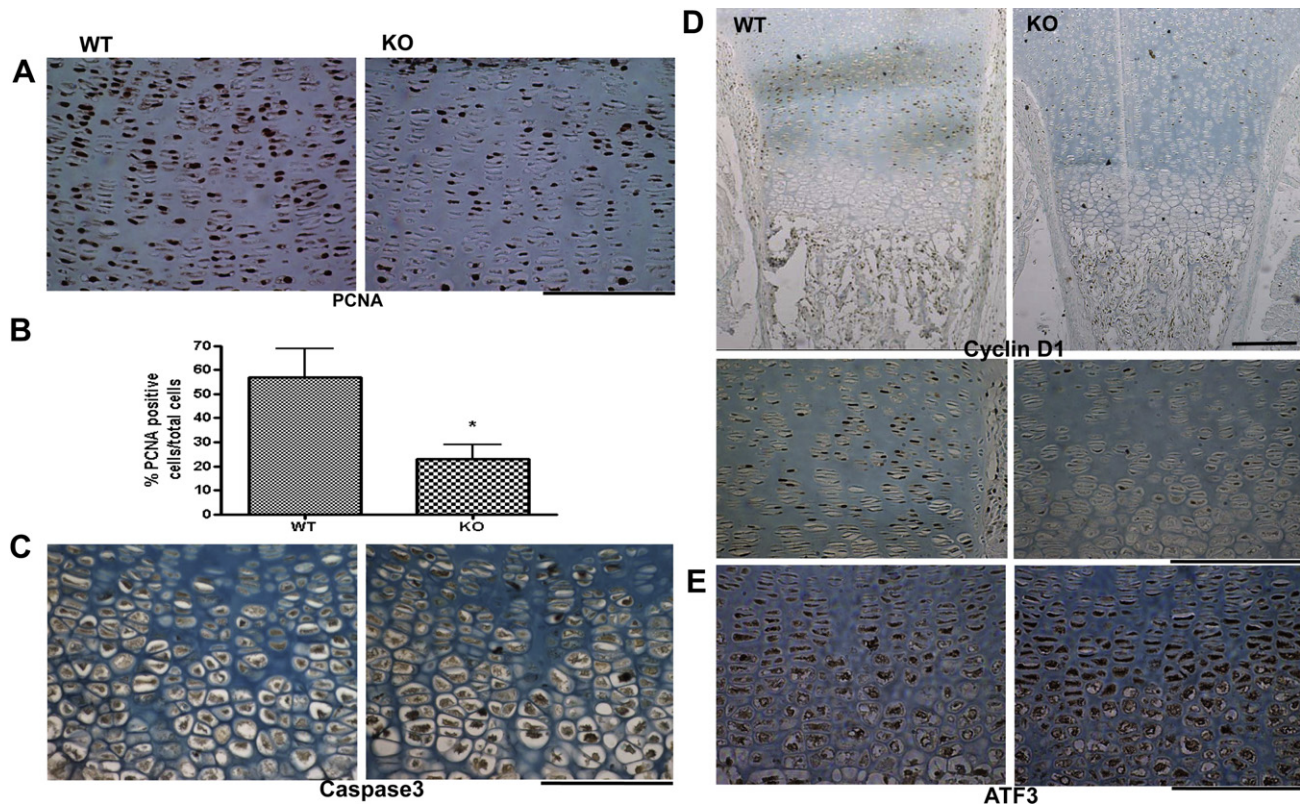


Fig. 3. *nNOS* deficiency reduces chondrocyte proliferation and increases apoptosis. Immunohistochemical staining of newborn tibia sections for proliferating cell nuclear antigen (PCNA; A) showed a reduction in stained cells in mutant mice, which was confirmed by cell counts (B); at least six mice per genotype are shown (* $P < 0.05$; mean \pm 95% confidence interval). Increased staining for cleaved caspase 3 was found in hypertrophic chondrocyte in mutant tibia sections (C). In addition, immunohistochemistry showed that less cells expressed cyclin D1 (D) while expression of ATF3 protein was increased (E) in growth plates from newborn mutant mice (C) (Scale bar = 200 μ m). Representative pictures from at least three independent experiments are shown.

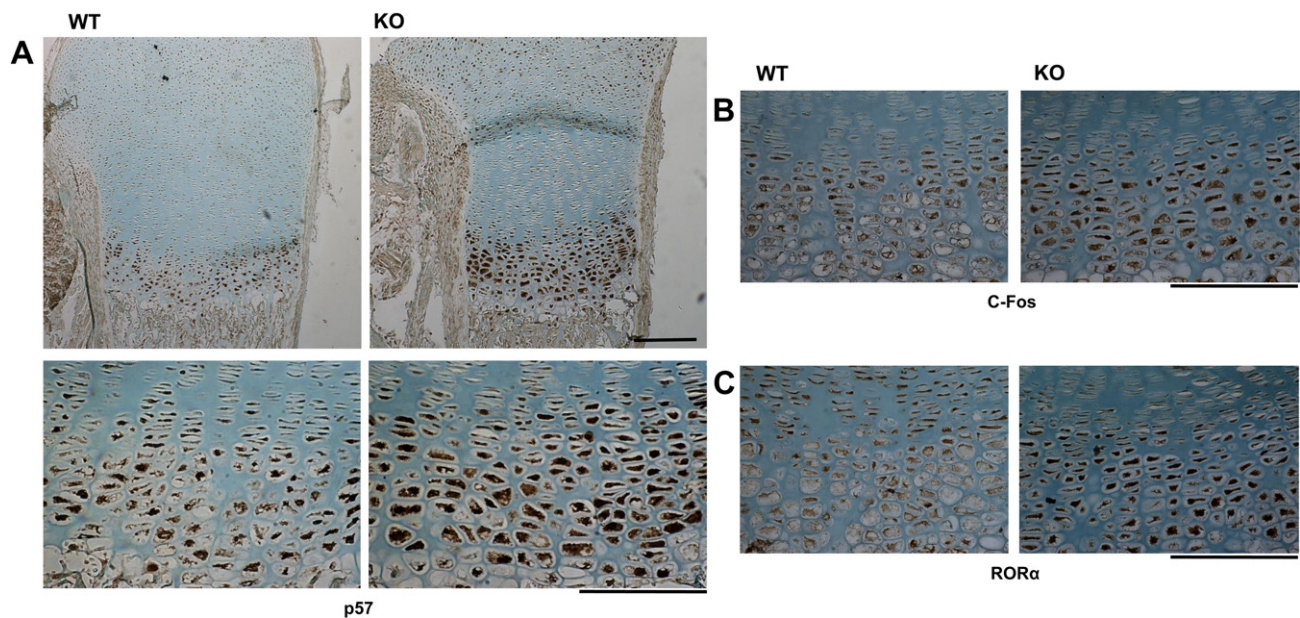


Fig. 4. Increased expression of early hypertrophic markers in *nNOS*-deficient chondrocytes. Expression of the cell-cycle inhibitor p57, which promotes cell cycle exit and is required for normal chondrocyte differentiation, was found increased in mutant mice by immunohistochemical analyses of newborn tibia sections (A). Immunohistochemistry also showed a similar increase in the number of cells expressing the transcription factors *c-fos* (B) and *RORα* (C) in sections from newborn mutants (Scale bar = 200 μ m). Representative pictures from at least three independent experiments are shown.

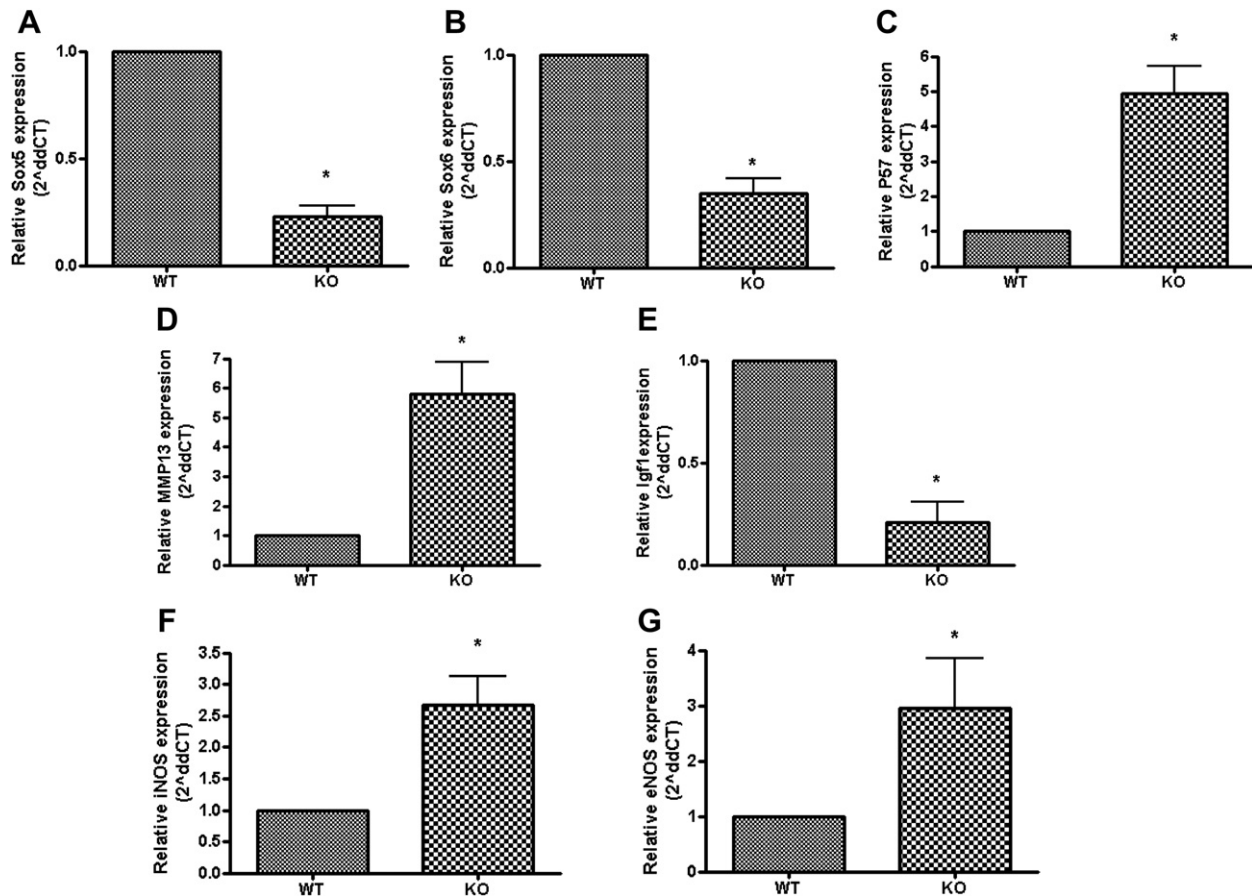


Fig. 5. *nNOS* deficiency affects cartilage-specific gene expression. Real-time RT-PCR revealed decreased expression for *Sox5* and *Sox6* transcripts (A, B) and increased expression of mRNA levels for *p57* and *Mmp13* (C, D) in cartilage of KO mice. Transcript levels for *Igf1* were significantly decreased in the mutant mice (E). mRNA levels of *iNOS* and *eNOS* were also found upregulated in *nNOS* KO cartilage (F, G). At least four independent experiments per genotype are shown (* $P < 0.05$; mean \pm 95% confidence interval).

potential explanation for this difference is that during hypertrophy, when all three NOS genes are expressed highly⁷, *eNOS* and/or *iNOS* (or potentially *CNP*) can compensate for the loss of *nNOS*, while they may not be able to do so in the proliferating zone.

The growth plate phenotype of *nNOS* KO mice is similar to that of *eNOS* and *iNOS* null mice^{17,18}. Given the similar functions the three NOS proteins and their similar expression in the growth plate⁷, the similarities between the phenotypes of the three KO lines were to be expected. In *eNOS* KO mice we only observed the upregulation of the *nNOS* gene, while *eNOS* and *iNOS* genes are both upregulated in *nNOS* KO mice. The compensatory regulation of transcripts of NOS enzymes may explain the relatively minor phenotype we observed in *nNOS* KO mice and provide further evidence for overlapping functions among NOS genes. It is likely that simultaneous inactivation of NOS genes would have more severe outcomes. However, it should be noted that mice lacking all three NOS genes have been described²⁸. Although those mice show a very high rate of lethality (85%), the surviving triple NOS KO mice live a surprisingly normal life²⁹, suggesting that additional compensatory mechanisms may exist.

nNOS inactivation results in reduced chondrocyte proliferation and increased apoptosis. However, increased staining for active caspase 3 was restricted to terminally differentiated hypertrophic chondrocytes, suggesting that apoptosis plays no or only a minor role in the reduced numbers of proliferating chondrocytes. Instead, one of the major reasons for the reduced proliferation appears to be the induction of the transcription factor *ATF3*, which is able to

suppress cyclin D1 transcription²⁵. Cyclin D1 expression is induced by many mitogenic stimuli and pathways in chondrocytes¹¹. Our studies suggest that in addition to positive regulation through transcription factors such as *ATF2* and *CREB*^{30–33}, cyclin D1 transcription is also under negative regulation by *ATF3*²⁵. The cyclin-dependent kinase inhibitor *p57* is a second cell cycle protein showing altered expression in the absence of *eNOS*, *iNOS* or *nNOS*. Immunohistochemistry showed earlier and broader expression in mutant mice, along with other prehypertrophic markers such as *RORα*. At the moment, it is unknown whether NO signaling regulates cyclin D1 and *p57* expression through a common pathway or through different effectors. It is also possible that premature differentiation to prehypertrophic chondrocytes is due to the reduced expression of *Sox5* and *Sox6* in *nNOS* KO cartilage, but the relationship between these transcription factors and cyclin D1 expression has not been addressed. Finally, reduced expression of *Igf1* could also contribute to the phenotype of *nNOS* KO mice, although the reduced growth in *Igf1*-deficient mice is largely due to smaller size of hypertrophic chondrocytes, as opposed to the primary effect on cell proliferation in our mice³⁴.

Loss of *nNOS* results in reduced von Kossa staining of cortical and trabecular bone. Picrosirius red staining suggests that this effect is due to paucity of trabecular structures *per se*, not just a delay in mineralization. At the moment, it is unclear whether this phenotype is secondary to defects in cartilage development or due to intrinsic functions of *nNOS* in osteoblasts or osteoclasts. Cell type-specific KO models will be required to resolve this question.

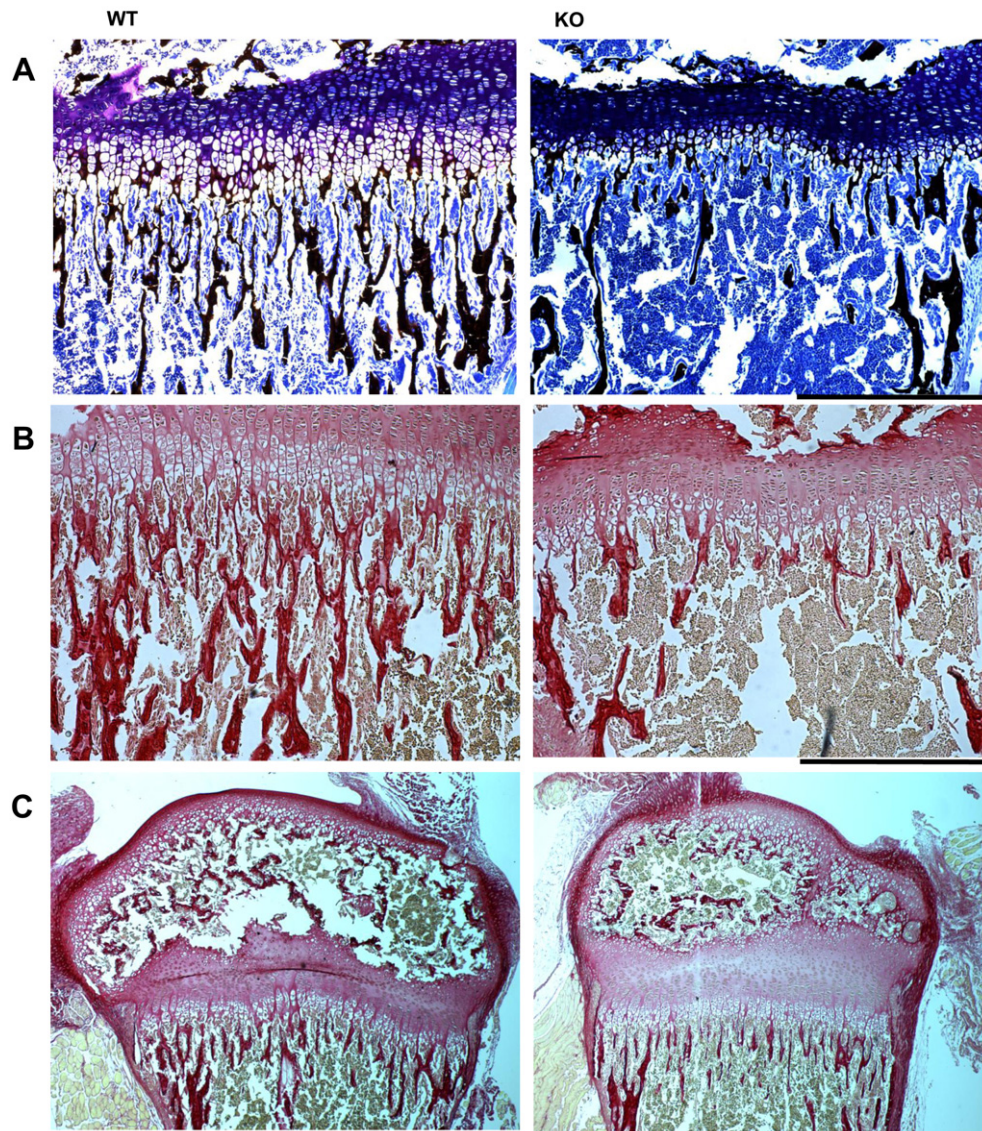


Fig. 6. *nNOS* deficiency leads to reduced trabecular bone and calcium deposition. Mineralization of trabecular and cortical bone shown by Von Kossa staining in tibia sections from postnatal day 21 mice was clearly decreased in mutant mice (A). A similar lack of trabecular structures was also seen by picrosirius red staining for fibrillar collagen (B). Secondary ossification centers were advanced in control mice at postnatal day 12, but delayed in mutant mice (C). (Scale bar: 200 μ m for A, B, D; 50 μ m for C) Representative pictures from at least three independent experiments are shown.

In summary, our data demonstrate a role for *nNOS* in chondrocyte proliferation apoptosis and maturation. Loss of *nNOS* affects numerous aspects of cartilage physiology, including chondrocyte proliferation and gene expression, as well as mineralization of bone. Reduced chondrocyte proliferation may in part be due to premature cell cycle exit shown by decreased cyclin D1 and increased p57 expression in mutants. It appears likely that the overall phenotype of *nNOS*-deficient mice is a combination of alternations in all these aspects. Further investigations into the specific mechanisms involved will result in a better understanding of physiological and pathological skeletal development and associated diseases, such as OA and osteoporosis.

Authors' contributions

QY carried out the experimental work, data collection and interpretation, and drafting the manuscript. QY and FB conceived of the study design and coordinated the studies and data

interpretation. Q.F. contributed mutant mice and consultation. All authors have read and approved the final manuscript.

Conflict of interest

The authors declare that they have no competing interest.

Acknowledgments

F.B. is a recipient of a Canada Research Chair. These studies were supported by funds from the Canadian Institutes of Health Research to F.B. (MOP 43899).

References

1. Murad F. Discovery of some of the biological effects of nitric oxide and its role in cell signaling. *Biosci Rep* 1999;19(3): 133–54.

2. Moncada S, Palmer RM, Higgs EA. Nitric oxide: physiology, pathophysiology, and pharmacology. *Pharmacol Rev* 1991; 43(2):109–42.
3. Teixeira CC, Agoston H, Beier F. Nitric oxide, C-type natriuretic peptide and cGMP as regulators of endochondral ossification. *Dev Biol* 2008;319(2):171–8.
4. Ignarro LJ. Nitric oxide: a unique endogenous signaling molecule in vascular biology. *Biosci Rep* 1999;19(2):51–71.
5. Abramson SB. Osteoarthritis and nitric oxide. *Osteoarthr Cartilage* 2008;16(Suppl 2):S15–20.
6. van't Hof RJ, Ralston SH. Nitric oxide and bone. *Immunology* 2001;103(3):255–61.
7. Teixeira CC, Ischiropoulos H, Leboy PS, Adams SL, Shapiro IM. Nitric oxide-nitric oxide synthase regulates key maturational events during chondrocyte terminal differentiation. *Bone* 2005;37(1):37–45.
8. Collin-Osdoby P, Nickols GA, Osdoby P. Bone cell function, regulation, and communication: a role for nitric oxide. *J Cell Biochem* 1995;57(3):399–408.
9. Drissi H, Zuscik M, Rosier R, O'Keefe R. Transcriptional regulation of chondrocyte maturation: potential involvement of transcription factors in OA pathogenesis. *Mol Aspects Med* 2005;26(3):169–79.
10. Karsenty G, Kronenberg HM, Settembre C. Genetic control of bone formation. *Annu Rev Cell Dev Biol* 2009;25:629–48.
11. Beier F. Cell-cycle control and the cartilage growth plate. *J Cell Physiol* 2005;202(1):1–8.
12. Horton WA. Skeletal development: insights from targeting the mouse genome. *Lancet* 2003;362(9383):560–9.
13. Provot S, Schipani E. Molecular mechanisms of endochondral bone development. *Biochem Biophys Res Commun* 2005; 328(3):658–65.
14. Zelzer E, Olsen BR. The genetic basis for skeletal diseases. *Nature* 2003;423(6937):343–8.
15. Dreier R. Hypertrophic differentiation of chondrocytes in osteoarthritis: the developmental aspect of degenerative joint disorders. *Arthritis Res Ther* 2010;12(5):216.
16. Pitsillides AA, Beier F. Cartilage biology in osteoarthritis—lessons from developmental biology. *Nat Rev Rheumatol* 2011;7(11):654–63.
17. Yan Q, Feng Q, Beier F. Endothelial nitric oxide synthase deficiency in mice results in reduced chondrocyte proliferation and endochondral bone growth. *Arthritis Rheum* 2010;62(7):2013–22.
18. Wang G, Yan Q, Woods A, Aubrey LA, Feng Q, Beier F. Inducible nitric oxide synthase-nitric oxide signaling mediates the mitogenic activity of Rac1 during endochondral bone growth. *J Cell Sci* 2011;124(Pt 20):3405–13.
19. van't Hof RJ, Macphee J, Libouban H, Helfrich MH, Ralston SH. Regulation of bone mass and bone turnover by neuronal nitric oxide synthase. *Endocrinology* 2004;145(11):5068–74.
20. Solomon LA, Li JR, Berube NG, Beier F. Loss of ATRX in chondrocytes has minimal effects on skeletal development. *PLoS One* 2009;4(9):e7106.
21. Wang G, Woods A, Agoston H, Ulici V, Glogauer M, Beier F. Genetic ablation of Rac1 in cartilage results in chondrodysplasia. *Dev Biol* 2007;306(2):612–23.
22. Ulici V, Hoenselaar KD, Agoston H, McErlain DD, Umoh J, Chakrabarti S, et al. The role of Akt1 in terminal stages of endochondral bone formation: angiogenesis and ossification. *Bone* 2009;45(6):1133–45.
23. Ulici V, Hoenselaar KD, Gillespie JR, Beier F. The PI3K pathway regulates endochondral bone growth through control of hypertrophic chondrocyte differentiation. *BMC Dev Biol* 2008;8:40.
24. Agoston H, Khan S, James CG, Gillespie JR, Serra R, Stanton LA, et al. C-type natriuretic peptide regulates endochondral bone growth through p38 MAP kinase-dependent and -independent pathways. *BMC Dev Biol* 2007;7:18.
25. James CG, Woods A, Underhill TM, Beier F. The transcription factor ATF3 is upregulated during chondrocyte differentiation and represses cyclin D1 and A gene transcription. *BMC Mol Biol* 2006;7:30.
26. Riemer S, Gebhard S, Beier F, Poschl E, von der Mark K. Role of c-fos in the regulation of type X collagen gene expression by PTH and PTHrP: localization of a PTH/PTHrP-responsive region in the human COL10A1 enhancer. *J Cell Biochem* 2002;86(4): 688–99.
27. Chusho H, Tamura N, Ogawa Y, Yasoda A, Suda M, Miyazawa T, et al. Dwarfism and early death in mice lacking C-type natriuretic peptide. *Proc Natl Acad Sci U S A* 2001;98(7): 4016–21.
28. Sabanai K, Tsutsui M, Sakai A, Hirasawa H, Tanaka S, Nakamura E, et al. Genetic disruption of all NO synthase isoforms enhances BMD and bone turnover in mice in vivo: involvement of the renin-angiotensin system. *J Bone Miner Res* 2008;23(5):633–43.
29. Nakata S, Tsutsui M, Shimokawa H, Suda O, Morishita T, Shibata K, et al. Spontaneous myocardial infarction in mice lacking all nitric oxide synthase isoforms. *Circulation* 2008;117(17):2211–23.
30. Beier F, Lee RJ, Taylor AC, Pestell RG, LuValle P. Identification of the cyclin D1 gene as a target of activating transcription factor 2 in chondrocytes. *Proc Natl Acad Sci USA* 1999;96(4):1433–8.
31. Beier F, Ali Z, Mok D, Taylor AC, Leask T, Albanese C, et al. TGFbeta and PTHrP control chondrocyte proliferation by activating cyclin D1 expression. *Mol Biol Cell* 2001;12(12): 3852–63.
32. Beier F, LuValle P. The cyclin D1 and cyclin A genes are targets of activated PTH/PTHrP receptors in Jansen's metaphyseal chondrodysplasia. *Mol Endocrinol* 2002;16(9):2163–73.
33. Ionescu AM, Schwarz EM, Vinson C, Puzas JE, Rosier R, Reynolds PR, et al. PTHrP modulates chondrocyte differentiation through AP-1 and CREB signaling. *J Biol Chem* 2001;276(15):11639–47.
34. Wang J, Zhou J, Bondy CA. Igf1 promotes longitudinal bone growth by insulin-like actions augmenting chondrocyte hypertrophy. *Faseb J* 1999;13(14):1985–90.
35. Woods A, Wang G, James CG, Dupuis H, Beier F. Microarray analyses of chondrocyte gene expression in response to manipulation of the actin cytoskeleton: Identification of a central role of RORα signaling. *J Cell Mol Med* 2009;13(9B): 3497–516.